Article

Water Dynamics and Structure of Highly Concentrated LiCl Solutions Investigated Using Ultrafast Infrared Spectroscopy

Sean A. Roget, Kimberly A. Carter-Fenk, and Michael D. Fayer*

Cite This: *J. Am. Chem. Soc.* 2022, 144, 4233−4243

Read Online

ACCESS | Metrics & More | Article Recommendations

ABSTRACT: In highly concentrated salt solutions, the water hydrogen bond (H-bond) network is completely disrupted by the presence of ions. Water is forced to restructure as dictated by the water−ion and ion−ion interactions. Using ultrafast polarization-selective pump−probe (PSPP) spectroscopy measurements of the OD stretch of dilute HOD, we demonstrate that the limited water−water H-bonding present in concentrated lithium chloride solutions (up to four waters per ion pair) is, on average, stronger than that occurring in bulk water. Furthermore, information on the orientational dynamics and the angular restriction of water H-bonded to both water oxygens and chloride anions was obtained through analysis of the frequency-dependent anisotropy decays. It was found that, when the salt concentration increased, the water showed increasing restriction and slowing at frequencies correlated with strong H-bonding. The angular restriction of the water molecules and strengthening of water−water H-bonds are due to the formation of a water−ion network not present in bulk water and dilute salt solutions. The structural evolution of the ionic medium was also observed through spectral diffusion of the OD stretch using 2D IR spectroscopy. Compared to bulk water, there is significant slowing of the biexponential spectral diffusion dynamics. The slowest component of the spectral diffusion (13 ps) is virtually identical to the time for complete reorientation of HOD measured with the PSPP experiments. This result suggests that the slowest component of the spectral diffusion reflects rearrangement of water molecules in the water−ion network.
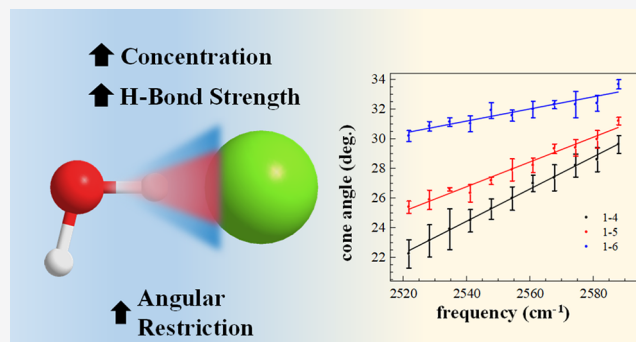
1. INTRODUCTION

The dynamical interactions between water and ions are of fundamental importance to many chemical and biological processes. Water is known to have many unique physical characteristics due to its extensive hydrogen bond (H-bond) network. The solvation of ions reorganizes this network, affecting many of water's properties, including its conductivity, viscosity, molecular diffusion, and its ability to solvate molecules such as proteins.[1] Basic knowledge of the effects of ions on the structure and dynamics of water aids in the understanding of a broad range of processes that occur in nature and in the development of new technologies.

For many years, aqueous salt solutions have been examined through a variety of techniques including Raman,[2] NMR,[3] and dielectric relaxation spectroscopy,[4] X-ray and neutron scattering, and molecular dynamics simulations.[5] Of the many experimental techniques, ultrafast infrared (IR) spectroscopy provides the sensitivity and time resolution for the measurement of structural dynamics in aqueous salt solutions. The effects of ions on the structure and dynamics of water have been directly observed by performing ultrafast IR experiments on the OD vibrational stretch of dilute HOD in solution. These experiments provided details on the general impact of the presence of the cation and anion, specific ion effects, and the extent to which water−ion interactions propagate in solution.[6−14] Ionic probes such as SCN^-, NO_3^-, and CO_3^- have also been used to examine structural dynamics from the perspective of the ion as well as investigate the formation and structure of ion pairs and clusters.[15−18]

Highly concentrated salt solutions have been receiving increasing attention due to their potential use as electrolytes in energy storage devices.[19−21] "Water-in-salt" electrolytes are a safer, more environmentally friendly alternative to organic solvents used in conventional Li^+-ion batteries and also have a larger stability window than their dilute "salt-in-water" counterparts.[22−24] These electrolytes typically have around 2−3 water molecules per ion pair and contain an inorganic cation like Li^+, Na^+, or Zn^{2+} and a larger, organic anion.[22−27]
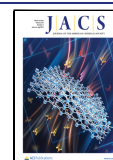
Other highly concentrated salt solutions are relevant to the chemical processing of materials, such as aluminum and radioactive waste.[28−30] At these concentrations, the structure of water is very different from that of the bulk liquid. While water typically forms ∼4 H-bonds with other water molecules giving rise to a tetrahedral H-bond network,[31,32] in concentrated salt solutions, most of these bonds are dedicated to solvating the ions, completely disrupting the H-bond network. Moreover, there is not enough water to fully solvate the ions, leading to the formation of contact and water-mediated ion pairs and aggregates in solution.[33,34] At extremely high salt concentrations studied here, extended salt/water networks are probably a better description for the ionic system.

Lithium chloride (LiCl) is an excellent system for investigating concentrated electrolyte solutions as it is a simple halide salt that has solubility just below three water molecules per ion pair. X-ray and neutron diffraction, in combination with molecular dynamics simulations, have been used to examine the restructuring and ion clustering that occur in aqueous LiCl solutions.[5,34−36] Recently, the structural dynamics of water and ions in aqueous LiCl solutions were observed via two-dimensional infrared (2D IR) spectral diffusion experiments on the nitrile stretch of the neutral organic probe, methyl thiocyanate (MeSCN).[37] This required careful analysis of the 2D line shapes from the 2D IR experiment as MeSCN undergoes chemical exchange processes between its interactions with water and the Li$^+$ cation, which complicates the extraction of spectral diffusion dynamics from the experiment.[38] Spectral diffusion of the CN stretch of MeSCN showed a component of ∼40 ps, which was interpreted as the time for water−ion network randomization. The CN stretch has a strong, well-documented first-order Stark coupling.[39−41] The Stark effect and the long nitrile vibrational lifetime make the spectral diffusion of the CN stretch sensitive to the relatively slow changes in electric fields associated with the water−ion network randomization.

Here, we present a complimentary study to provide direct information on the water structure and dynamics present in concentrated LiCl solutions by looking directly at water through measurements of the OD stretch of dilute HOD. In addition to the spectral diffusion dynamics measured via the 2D IR experiments, direct information on the water reorientation and H-bond structure is obtained from polarization-sensitive pump−probe (PSPP) experiments. These experiments reveal additional aspects of the structure and dynamics of the highly concentrated solutions through water H-bond interactions with both water and chloride anions that result in restricted angular motions.

2. EXPERIMENTAL METHODS

2.1. Sample Preparation. LiCl (anhydrous, >99%) was purchased from Sigma-Aldrich and used without further purification. LiCl was stored in a dry box purged of water vapor until ready for use. LiCl aqueous solutions were prepared in molar ratios of 1−4, 1−5, and 1−6 LiCl to H_2O. Solutions were also prepared with 5% HOD in H_2O for use in the nonlinear experiments. The solutions were sandwiched between two CaF_2 windows, 1 in. diameter, separated by a Teflon spacer that was 12 μm thick. Linear IR absorption spectra were measured using a Thermo Scientific iS50 FTIR spectrometer with a resolution setting of 0.5 cm^{-1}. The chamber of the spectrometer was purged to minimize background absorption from IR-active atmospheric gases, such as carbon dioxide and water vapor. Solutions prepared with H_2O were used to isolate the linear spectrum

of the OD stretch in the aqueous salt solutions via background subtraction.

2.2. Laser System and Nonlinear IR Experiments. The nonlinear experiments were performed using a laser system that has been described previously in detail.[42] Briefly, a Ti:Sapphire oscillator/regenerative amplifier system was used to pump an optical parametric amplifier to generate mid-infrared pulses, centered at ∼4 μm with a pulse duration of ∼65 fs. The pulses are then split into 2 or 4 pulses and passed through an interferometric system of precision delay stages. The pulses are focused and crossed in the sample using off-axis parabolic reflectors to generate the nonlinear signal of interest. The signal is frequency-resolved and heterodyne-detected using a monochromator equipped with a 32 pixel mercury cadmium telluride array detector configured as a spectrograph.

For the PSPP experiments, the pulse is split into a strong pump pulse and a weaker probe pulse. The pump pulse is linearly polarized +45° relative to the probe pulse, which is horizontally polarized (0°). Immediately after the sample, a computer-controlled polarizer is used to resolve the nonlinear signal either parallel (+45°) or perpendicular (−45°) to the pump pulse and a second polarizer just prior to the monochromator is used to return the signal polarization to 0°. This polarization scheme enables the detection of the parallel and perpendicular signals in a manner that avoids polarization bias from the diffraction grating in the spectrograph. The parallel and perpendicular signals, $S_{\parallel}(t)$ and $S_{\perp}(t)$, respectively, can be used to obtain the population relaxation, $P(t)$, and the anisotropy, $r(t)$, which is related to the second-order Legendre polynomial orientational correlation function, $C_2(t)$, using the following equations:

$$P(t) = [S_{\parallel}(t) + 2S_{\perp}(t)]/3 \tag{1}$$

$$r(t) = \frac{S_{\parallel}(t) - S_{\perp}(t)}{S_{\parallel}(t) + 2S_{\perp}(t)} = 0.4C_2(t) \tag{2}$$

The relaxation of the vibrational energy absorbed by the OD stretch of HOD also induces an isotropic, long-lived, heating signal in the PSPP experiment. To accurately measure the observables of interest, the heating signal was removed using a well-documented procedure.[43,44]

In the 2D IR experiments, the IR pulse is split into three pump pulses and a local oscillator (LO) pulse. The three pulses are crossed in the box-CARS geometry, generating a nonlinear, echo signal in a distinct, but known, direction. The nonlinear signal is then overlapped with the LO pulse for heterodyne detection. In this experiment, the first two pulses label and store the initial frequencies of the probe molecules. After a delay, T_w, following the second pulse, the third pulse generates a vibrational echo, which reports the final frequencies of the probe molecules after structural evolution of the system occurs during the T_w period. Scanning the time delay, τ, between pulses 1 and 2 produces interferograms at each frequency detected by the array. A numerical Fourier transformation of the interferograms gives data along the horizontal axis, ω_τ, in the 2D spectrum. The spectrograph frequency resolves the echo/LO pulse, acting as an experimental Fourier transform that generates data along the vertical axis, ω_m, in the 2D spectrum. For short T_w periods, the 2D line shape is elongated along the diagonal as the initial frequencies are significantly correlated with the final frequencies. For longer T_w, structural rearrangements in the ionic solution cause decorrelation of the initial and final frequencies, making the 2D line shape rounder. The change in shape with T_w is used to determine the time constants associated with the structural evolution of the system. The center line slope (CLS) method is used to determine the normalized frequency−frequency correlation function (FFCF), from which the complete FFCF is calculated.[45−47]

3. RESULTS AND DISCUSSION

3.1. Linear Spectra. The OD stretch of HOD in H_2O is sensitive to the wide range of H-bonding configurations present in the water H-bond network, as demonstrated by its

broad absorption spectrum shown in Figure 1. Within the vibrational spectrum, HOD molecules with stronger and/or
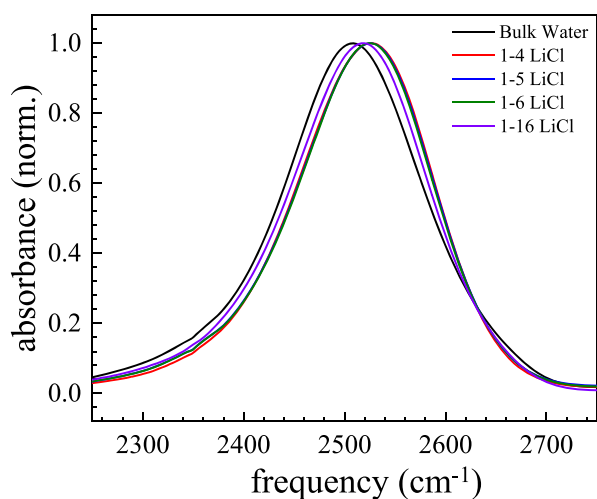
Figure 1. Background-subtracted and normalized absorption spectra of the OD stretch of HOD in bulk water and in aqueous LiCl solutions of concentrations 1−4, 1−5, 1−6, and 1−16 (ion pairs to water).

more water H-bonds are observed at lower frequencies (red shifted) while HOD molecules with weaker and/or fewer H-bonds are observed at higher frequencies (blue shifted). When salt is added, the pure water H-bond network reorganizes to solvate the ions. Water−ion interactions lead to a modification of the OD stretch spectrum. H-bonding between the anion and HOD has a significant effect on the position and width of the spectrum. Anion-associated water populations often appear on the high-frequency side of the vibrational spectrum resulting in an overall blue shift. This is because water−anion H-bonding is weak compared to water−water H-bonding due to the lower charge density of the anion. The water-halide H-bonding interaction have been characterized by measuring the absorption spectrum of the OD stretch of HOD in various halide salt solutions. It is observed that the mode shifts more toward higher frequencies as the charge density of the halide ion decreases.[48−50] Notably, fluoride is the only halide anion that leads to a red shift of the OD spectrum.[49−53] Large organic anions, like bistriflimide (NTf$_2^-$),[54,55] hexafluorophosphate (PF$_6^-$),[56,57] and tetrafluoroborate (BF$_4^-$),[8,58] which have very diffuse charges, give rise to large spectral shifts >+100 cm^{-1} with respect to the OD stretch spectrum in bulk water, which is centered at 2509 cm^{-1}. It was also found that the cation has a role in determining the OD stretch spectrum, though it is a more subtle effect.[13]

The absorption spectra of the OD stretch of HOD in concentrated LiCl solutions are shown in Figure 1. The small features around 2350 cm^{-1} are due to trace atmospheric CO$_2$ remaining in the FTIR sample compartment. As salt is added to the solution, the OD stretch spectrum increasingly shifts from 2509 to 2527 cm^{-1}. The shift is caused by the interaction between water and chloride anions (chloride-associated population), which arises from the solvation of LiCl. As the concentration of LiCl increases, the center of the overall spectrum approaches the center of the chloride-associated spectrum as it becomes a larger fraction of the water H-bonding interactions. This is shown in Figure 1, where the concentration increases from bulk water to an intermediate

concentration, 1−16, and then to high concentrations. The 1−6 to 1−4 concentrations are virtually identical though the 1−4 concentration shows very slight narrowing on the wings of the spectrum.

When there is a large spectral shift caused by the water−anion H-bonding interaction, the anion-associated spectrum can be resolved from the water-associated spectrum and their characteristics can be determined through peak fitting. However, due to the small spectral shift caused by the chloride anion, demonstrated by the ∼20 cm^{-1} shift in the overall spectrum at the highest concentrations, it is not possible to separate the anion-associated spectrum using the linear spectra. To resolve the water−chloride and water−water spectral features, the differences in the vibrational lifetimes of the two species were employed, as described in the next section.

3.2. Vibrational Relaxation. The population decays calculated from the PSPP experiments (eq 1) are measurements of the vibrational relaxation of the probe molecule to the ground state following excitation. The vibrational lifetime quantifies how quickly the energy absorbed by the vibrational mode is dissipated into lower energy intramolecular and bath modes.[59] Vibrational relaxation is thus sensitive to the coupling of the probe to its surrounding environment. If there are distinct local interactions between the probe and the medium, then there can be differences in the coupling of the vibrational energy to the bath, giving rise to multiexponential population decays.

The normalized frequency-dependent population decays of the OD stretch of HOD in 1−5 LiCl solution are shown in Figure 2. The vibrational relaxation at each frequency fits well
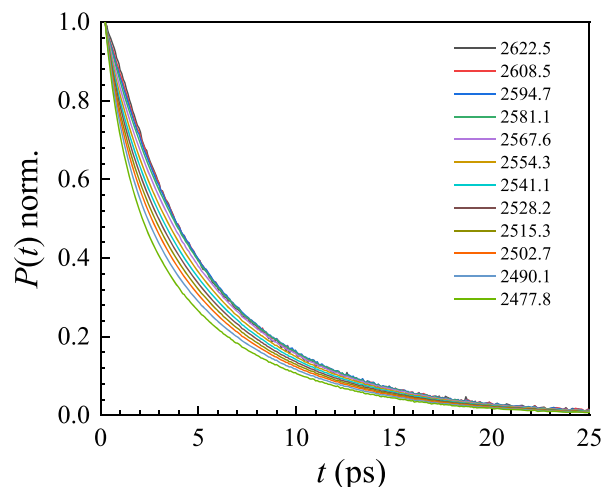
Figure 2. Normalized, frequency-dependent vibrational relaxation of the OD stretch of HOD in 1−5 LiCl aqueous solution.

to a biexponential decay, indicating that there are two distinguishable populations present in the salt solution. The two decay components are from the presence of both water−water and water−chloride H-bonding as discussed in the previous section. The lifetimes of these populations for the different concentrations are provided in Table 1. Based on previous findings, the fast component can be attributed to the water-associated population, while the slow component is the chloride-associated population.[6,12,13] The longer time constant reflects a weaker coupling of the OD stretch vibrational mode to the medium and is much longer than that observed in pure

Table 1. Observed Lifetimes from Fits to the Population Decays of the OD Stretch of HOD in Bulk Water and in Aqueous LiCl Solutions[a]

solution	t_w	t_a
1–4	1.3 ± 0.1	6.4 ± 0.1
1–5	1.1 ± 0.1	5.5 ± 0.1
1–6	1.0 ± 0.1	5.2 ± 0.1
bulk water	1.8 ± 0.1	

[a]t_w—lifetime of the water-associated population and t_a—lifetime of the anion-associated population.

water. In the more extreme case of dilute water (isolated water molecules) in a room temperature ionic liquid, the lifetime of the anion-associated water is tens of picoseconds long.[54] With increasing concentration of salt, there is an observable increase in the lifetime of the anion-associated population, while the lifetime of the water-associated population was observed to be independent of the concentration over the range studied but slightly faster than the lifetime of HOD in bulk water.

The frequency-dependent amplitudes determined from the biexponential fits are shown in Figure 3. These amplitudes map
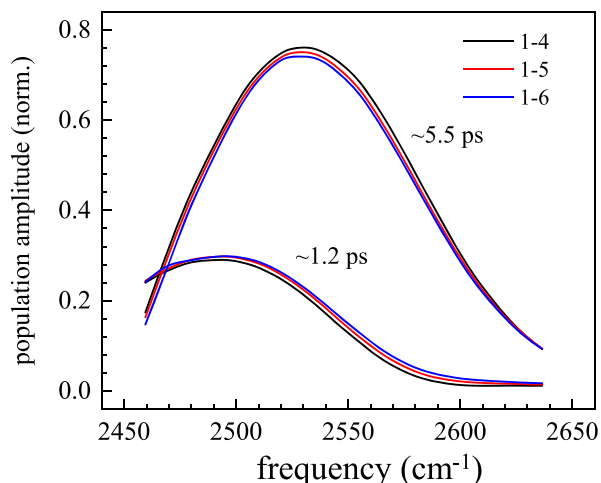

Figure 3. Frequency-dependent population amplitudes at $t = 0$ of the water-associated and chloride-associated HOD populations determined from the biexponential curve fitting of the vibrational relaxation as described in the text.

out the contributions of the water−water and water−chloride H-bonds to the overall OD stretch absorption spectrum. The amplitudes are normalized to the maximum value of the overall pump−probe signal, similar to the normalized linear spectra shown in Figure 1. Due to the difference of the vibrational lifetimes of the two species, the overlapping contributions can be separated into individual component spectra. The frequency range is limited at the lower frequencies due to the presence of the 1−2 transition, which is a result of excited-state absorption in the third-order nonlinear experiment. In contrast, the 0−1 transition is a result of ground-state bleach and stimulated emission. Therefore, these two transitions occur with opposite signs and cancel each other where they overlap in frequency. Moreover, the 0−1 and 1−2 transitions relax with the same vibrational lifetime; thus, they cannot be resolved through multiexponential fitting.

As noted in the previous section and shown in Figure 3, the chloride-associated population (with the longer lifetime) is

shifted to higher frequencies compared to bulk water due to weaker H-bonding between water and the chloride anion. A Gaussian fit to the water−chloride spectrum indicates that it is centered at 2530 cm^{-1}, slightly higher than the center of the total linear absorption spectrum (Figure 1). The shape of the water−chloride spectrum is largely unchanged with concentration, though, like the linear spectra, the highest concentration has some narrowing on the wings of the transition. It is also observed that the water−water spectrum is shifted to lower frequencies (2492 cm^{-1}), compared to bulk water (2509 cm^{-1}), and the shape and position remain virtually identical for the concentrations studied. The water−water component of the 1−5 LiCl solution is compared to the frequency-dependent amplitudes from population decays of HOD in bulk water in Figure 4. The spectral shift of the water-associated population
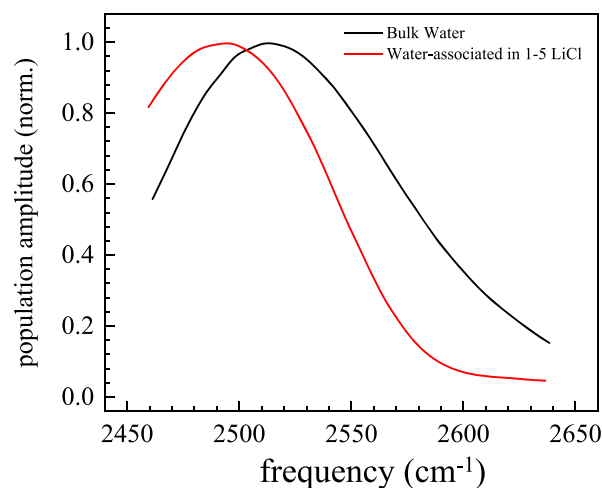
Figure 4. Comparison of the OD stretch water-associated population amplitudes of the 1−5 LiCl aqueous solution and bulk water.

in the salt solutions indicates that the H-bonding interaction is stronger, on average, than that observed in bulk water. A red shift also occurs when a water hydroxyl H-bonds to a fluoride anion, though the shift is even larger for fluoride. The fluoride-associated population shows a spectral shift of the OD stretch, which is ∼ −60 cm^{-1} (∼2450 cm^{-1}).[51,52] This frequency shift is often attributed to fluoride being a "structure-making" ion in the Hofmeister series, whereas the other halides are borderline, if not "structure-breaking" ions. However, since the red shift is observed in the water-associated population of the LiCl solution, the enhanced H-bond strength is more comparable to the water interactions found in ice, which has a highly ordered H-bond network.[60,61]

Molecular dynamics (MD) simulations have indicated that in highly concentrated LiCl solutions, there are many contact ion pairs and clusters as well as solvent-shared and solvent-separated ion pairs[5,34,35] (While the term clusters is frequently used in the literature, there is a continuous network of water and ions with different local arrangements). Thus, it can be concluded that the frequency shift of the water−water spectrum is due to the formation of larger water−ion structures that foster stronger interactions between the water molecules. Most of the water−water interactions that occur in these solutions are of the form of solvent-separated ion pairs, where two water molecules act as a bridge between oppositely charged ions. Formations such as these can possibly strengthen an H-bond by increasing the partial charges of the H-bond

donor and acceptor through electrostatic interactions between the water lone pairs and the ions. Evidence of such interactions was found in recent classical MD simulations, where strengthening of the H-bond shared between water molecules in the first and second solvation shells of ions was observed when the H-bond donor is directly interacting with the cation or the H-bond acceptor is directly interacting with an anion.[62]

3.3. Orientational Relaxation. The anisotropy calculated from the PSPP experiments, as described in eq 2, is a measure of the water orientational dynamics. It is proportional to the second-order Legendre polynomial orientational correlation function, $C_2(t)$, which describes the decorrelation of the orientation of the transition dipole (OD bond vector) as the probe reorients in angular space. At time, $t = 0$, the initial anisotropic orientational distribution of OD bonds excited by the pump pulse and their final orientations are perfectly correlated, giving an anisotropy value of 0.4. As time proceeds, the OD bonds reorient, leading to complete decorrelation once the ensemble of HOD molecules has sampled all angles, corresponding to an anisotropy value of 0. Although the OD bond direction is measured in the experiment, orientational relaxation requires reorientation of the entire HOD molecule. In the bulk liquid, water reorients via jump reorientation, which involves the concerted rearrangement of many water molecules.[63] While the OD vibrational frequency and lifetime are principally determined by the local interactions of the OD bond, the reorientation of HOD is more global, likely involving multiple ions and water molecules.

The anisotropy decays of HOD in the LiCl solutions near the center frequency are shown in Figure 5. The experimental
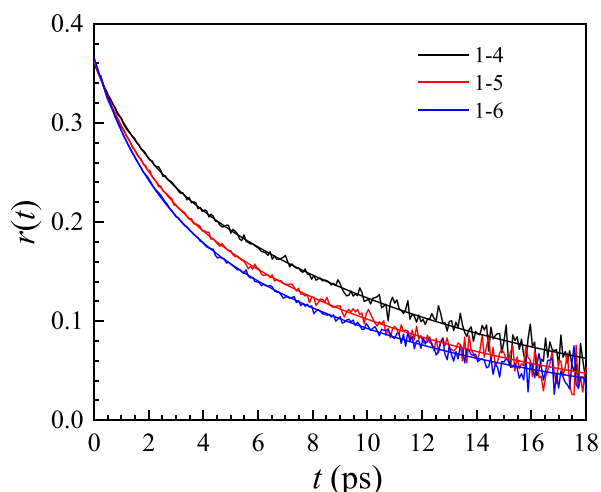
Figure 5. Anisotropy decays of the OD stretch of HOD in aqueous LiCl solutions at 2527 cm^{-1}.

data begin at ~250 fs because the finite pulse duration of the overlapping pump and probe pulses generates a strong, nonresonant signal from the sample that obscures the data at short time delays. The frequency-dependent anisotropy decays of each concentration were fit to biexponential functions, sharing the time constants across all frequencies. Fitting the decays at each frequency individually yielded time constants that were the same within the experimental error. The results of the curve fitting are given in Table 2. When the fits are extrapolated back to $t = 0$, the decays begin slightly below 0.4. This is due to the fast inertial motions (<100 fs) of the water molecules, which have time dependence that cannot be experimentally resolved because of the pulse duration.[64]

The orientational relaxation of HOD in bulk water fits well to a single exponential decay with a reorientation time constant of 2.6 ps.[6,44] In the LiCl solutions, the orientational dynamics are much slower than those observed in bulk water and have two timescales for reorientation. These two time constants can be understood using the wobbling-in-a-cone model.[65−67] The first time constant, t_1, describes reorientation in a restricted angular space defined by a cone of half-angle, θ_c. The second, longer time constant, t_2, describes the complete angular diffusion occurring following the release of constraints that restricted the short time angular motion. When wobbling-in-a-cone dynamics occur, the orientational correlation function is given by:

$$C_2(t) = [S_2^2 + (1 - S_2^2)\exp(-t/t_c)]\exp(-t/t_m) \quad (3)$$

where t_c is the restricted (cone) angular diffusion time constant, t_m is the complete (free) angular diffusion time constant ($t_m = \frac{1}{6D_m}$, where D_m is the orientational diffusion constant), and S_2 is the generalized order parameter given by:

$$S_2 = \frac{1}{2}\cos\theta_c(1 + \cos\theta_c) \quad (4)$$

The orientational correlation time constants in the wobbling-in-a-cone model are related to the time constants t_1 and t_2 of the biexponential decay by $t_c = (t_1^{-1} - t_2^{-1})^{-1}$ and $t_m = t_2$. The restricted angular diffusion constant, D_c, depends on both t_c and θ_c and can be described for $\theta_c < 30°$ as

$$D_c \cong \frac{7\theta_c^2}{24t_c} \quad (5)$$

In the results presented, the full expression for any cone angle is used to calculate the diffusion constant as described in the literature although the differences from the use of eq 5 are negligible.[67]

For the concentrations studied, the time constants from the biexponential fit to the anisotropy do not vary, giving a wobbling time, $t_c = 2$ ps, and a free diffusion time constant, $t_m = 12$ ps. The free diffusion reorientation is noticeably slower

Table 2. Fit Parameters for the Anisotropy of the OD Stretch of HOD in Bulk Water and Aqueous LiCl Solutions Using the Wobbling-in-a-Cone Analysis for Restricted Orientational Relaxation

solution	t_1	t_c	D_c^{-1} (ps)^{a,b}	θ_c (slope)^a	$t_m = t_2$ (ps)	D_m^{-1} (ps)
1−4	1.6 ± 0.2	1.9 ± 0.2	34 ± 6	26 (0.11)	12 ± 1	72 ± 6
1−5	1.6 ± 0.1	2.0 ± 0.2	30 ± 4	28 (0.08)	10 ± 1	60 ± 6
1−6	1.8 ± 0.1	2.2 ± 0.2	28 ± 1	32 (0.04)	11 ± 1	66 ± 6
bulk water					2.6 ± 0.1	15.6 ± 0.6

^{a}Average across all frequencies. ^{b}Error bars are the standard deviation across all frequencies.

than that in bulk water, which is in line with previous measurements of aqueous salt solutions.[6,12,13] Even though the time constants are essentially identical at each concentration, it is evident that there are differences in the shapes of the decays caused by changes in the wobbling cone angle, θ_c, with concentration. The frequency-dependent cone angles are presented in Figure 6. As the salt concentration is reduced,
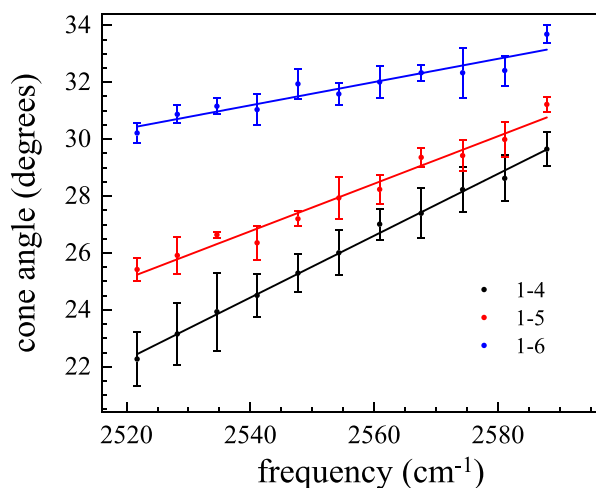
Figure 6. Frequency-dependent cone angles determined from the wobbling-in-a-cone analysis of the anisotropy decays of HOD in aqueous LiCl solutions. Error bars are the standard deviation after analyzing three individual experiments for each concentration. Solid lines are linear fits to the cone angles at each concentration.

there is an overall increase in the cone angles across all frequencies, implying that there is more freedom to reorient at short times when the H-bonds are intact for the more dilute salt solutions. Figure 6 also shows that the frequency dependence of the cone angles vary with concentration. The change in cone angles with frequency is well described by a linear fit. As the concentration decreases, the slope of the cone angles with frequency also decreases. The time constants and diffusion constants are given in Table 2 as well as the average cone angle and the slope for each LiCl solution.

As described in the previous section, the frequency is correlated to the strength of the OD H-bond. At the highest concentration studied, there is a wide range of cone angles observed for different H-bond strengths, with the HOD molecules with strong H-bonds (lower frequencies) being more restricted than those with weaker H-bonds. As the concentration decreases (see Figure 6), there is a much smaller range of angles, decreasing from ~7° for the 1−4 concentration to ~3° for the 1−6 concentration over the same frequency range (range of H-bond strengths). Furthermore, since t_c is frequency-independent, the diffusion constant, D_c, follows the same trends (see eq 5); there is a wider range of cone orientational diffusion constants at higher concentrations, with smaller diffusion constants observed for stronger H-bonds. At lower concentrations, the cone orientational diffusion constants vary much less with the H-bond strength (frequency).

Though wobbling-in-a-cone dynamics have been reported for HOD in a range of salt solutions,[6,12,13,19] frequency dependence of the cone angles has not been reported for simple salt solutions. Most simple salts have limited solubility, so it is possible that the large frequency dependence observed

here, which becomes relatively small by a 1−6 molar ratio, may not have been present in previous studies. A wide range of cone angles have been observed for 1−2.5 LiNTf$_2$ solution (ion pairs per H$_2$O) and 1−0.66 EmimNTf$_2$ ionic liquid in agreement with the 1−4 LiCl results presented here, but no concentration-dependent studies were performed.[55] This suggests that it is possible that the frequency dependence is present for other highly concentrated salt solutions. For 1-alkyl-3-methylimidazolium tetrafluoroborate ionic liquids of various alkyl chain lengths, while there was a strong variation in the cone angle across frequency, it was observed that the ratio of ion pairs to water did not have a significant effect on the frequency dependence.[58]

The concentration dependence indicates that the H-bond strength is not the only factor determining the cone angle. Another possible factor is steric hindrance in the salt solution from structural ordering induced by the high concentration of salts. Previous PSPP experiments of molecular probes confined in the free volume elements of amorphous polymers have been used to determine the size distribution of the free volume regions based on the variation of the cone angles.[68,69] Though water is not "confined" in a given space as in the polymers, it is not hard to visualize water angularly constrained by structural features such as ion crowding at these high concentrations. The simplest examples are water involved in solvent-shared and solvent-separated ion pairs. When acting as a bridge between Li$^+$ and Cl$^-$ ions, water is likely to be highly constrained, resulting in slow reorientation. The observed restructuring of the solution appears to have a large effect on the angular space available for water molecules undergoing strong H-bonding interactions. The observed restriction of the cone angles is likely due to the formation of extended water−ion network structures (extended aggregation) rather than ion pairs since MD simulations indicate that there is a significant number of ion pairs even at the lowest concentration studied here.

3.4. Spectral Diffusion. Spectral diffusion is the fluctuation of the vibrational frequency of a probe molecule's vibrational transition due to structural evolution of its surrounding environment. From the 2D IR experiment (described in Section 3), spectral diffusion dynamics can be measured from the time dependence of the 2D vibrational spectra. The change in shape of the 2D spectrum with T_w can be seen in Figure 7, which displays the 2D spectra of the OD stretch of HOD in the 1−5 LiCl solution at two times, $T_w = 1$ and 10 ps. In the figure, the red band along the diagonal (dashed line) corresponds to the 0−1 vibrational transition (which is generally used for analysis), while the blue band that is off-diagonal arises from the 1−2 transition. Spectral diffusion dynamics are obtained from analysis of the shape change of the 2D spectrum with T_w. This analysis is done using the CLS method, which gives the normalized FFCF.[45,46] The FFCF is the probability that the vibrational probe at an initial frequency (ω_τ) is at the same frequency at a later time (ω_m), averaged over all probe molecules. The CLS(T_w) decay begins at 1 and decays to zero at a sufficiently long time due to spectral diffusion (structural evolution).

The complete FFCF is typically described using the Kubo model:[70,71]
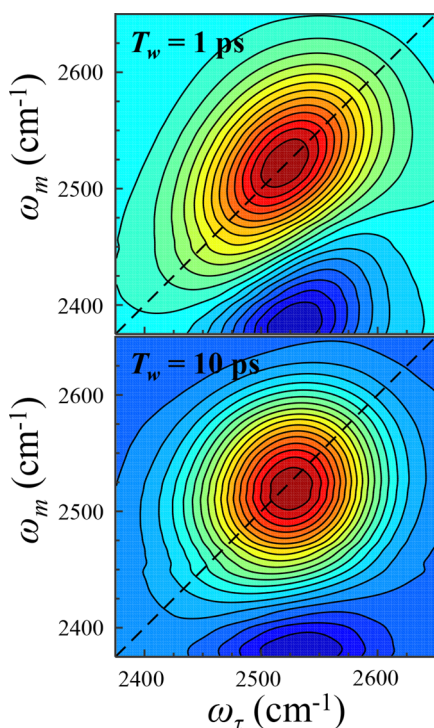
Figure 7. Representative 2D IR spectra of the OD stretch of HOD in 1−5 aqueous LiCl solution at two waiting times, T_w = 1 ps and 10 ps.

$$\text{FFCF} = C_\omega(t)\langle\delta\omega(0)^2\rangle = \langle\delta\omega(t)\delta\omega(0)\rangle$$
$$= \sum_i \Delta_i^2 \exp[-t/\tau_i] \tag{6}$$

where $\delta\omega(t) = \omega(t) - \langle\omega\rangle$ is the frequency fluctuation as a function of time, Δ_i is the frequency fluctuation amplitude, and τ_i is the decay time constant for the ith component of the frequency fluctuations. The homogeneous linewidth, $\Gamma = \frac{1}{\pi T_2}$, which has contributions from ultrafast dephasing processes as well as the vibrational lifetime and the orientational relaxation, can also be observed as the deviation of the CLS(0) value from 1. In the limit $\Delta_i\tau_i \ll 1$, the ith component is motionally narrowed and contributes to the homogeneous linewidth. Homogeneous dephasing in water systems usually dominates the homogeneous linewidth. By using both the CLS(T_w) decay and the linear absorption spectrum, the complete FFCF including the homogeneous linewidth can be determined.[45,46,72]

The CLS(T_w) decays of the OD stretch of HOD in the LiCl solutions are shown in Figure 8. These decays effectively reflect the spectral diffusion of the chloride-associated population because, as indicated by the population amplitudes (Figure 3) and the short lifetime (~1.2 ps), the water-associated population only makes a small contribution to the 2D IR signal. In addition, the CLS analysis is performed around the peak of the 2D spectrum, which is dominated by the chloride-associated population. Chemical exchange between the two populations is possible, which would result in the growth of off-diagonal peaks, and has been seen in 2D IR experiments of HOD in perchlorate and BF$_4^-$ salt solutions.[8,9] However, there is no evidence of off-diagonal exchange peaks, suggesting that the exchange processes occur on a timescale too long to be observed in the experiments. A biexponential function provides the best fits to the CLS(T_w) decays, demonstrating that
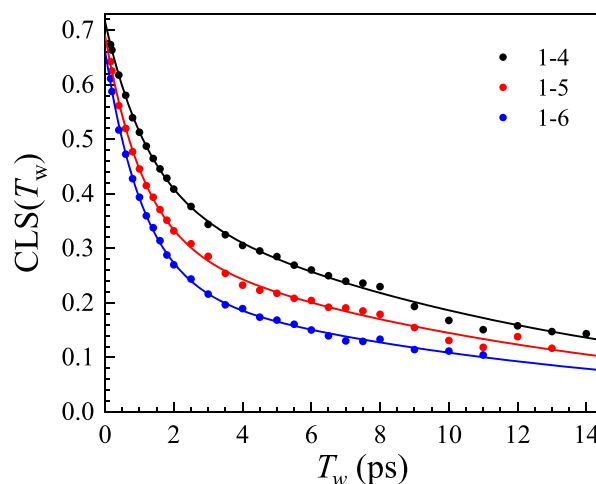
Figure 8. CLS(T_w) decays (points) and their corresponding fits (solid lines) for the OD stretch of HOD in aqueous LiCl solutions.

spectral diffusion occurs via two structural processes. The parameters for the full FFCF were calculated based on the fits and are presented in Table 3.

Table 3. Complete FFCF Parameters from the CLS Decays and the Linear Absorption Spectra[72] of the OD Stretch of HOD in Bulk Water and in Aqueous LiCl Solutions

sample	Γ (cm^{-1})	Δ_1 (cm^{-1})	τ_1 (ps)	Δ_2 (cm^{-1})	τ_2 (ps)
1−4	54 ± 5	35 ± 2	1.2 ± 0.1	43 ± 2	13 ± 1
1−5	55 ± 5	39 ± 2	1.1 ± 0.1	37 ± 2	13 ± 1
1−6	57 ± 4	41 ± 2	1.1 ± 0.1	32 ± 2	12 ± 1
bulk water	67 ± 4	43 ± 2	0.4 ± 0.1	31 ± 2	1.7 ± 0.1

The CLS(T_w) decay of HOD in bulk water also has two decay components with time constants of 0.4 and 1.7 ps (also presented in Table 3). MD simulations have shown that the fast time constant is mainly a result of fluctuations in the H-bond length with some contributions from angular fluctuations, while the slower time constant is a result of breaking and making H-bonds, which leads to complete randomization of the H-bond network.[73,74] With the addition of LiCl, it is likely that the structural processes remain the same but they are much slower, with a fast component of 1.2 ps and a slow component of 13 ps. The slowing of the spectral diffusion in concentrated LiCl solutions compared to pure water dynamics is in line with previous measurements of HOD in lower concentration aqueous salt solutions.[6,13] The time constants for the LiCl solutions are independent of concentration within the experimental error, and the main difference between the solutions is the amplitude of each component in the overall decay as quantified by the Δ_is presented in Table 3.

It is worth noting that the slow component of the anisotropy (Table 2) and the slow component of the CLS decay (Table 3) are essentially the same within the experimental error. Though the FFCF and $C_2(t)$ are different correlation functions, the same dynamical process, that is, the breaking and making of H-bonds through jump reorientation, is responsible for the decays in bulk water. The dynamical observables measured using the two experiments are not necessarily the same. For example, HOD in bulk water has a reorientation time of 2.6 ps while its slowest spectral diffusion

time constant is 1.7 ps. 2D IR experiments on HOD in lower concentration salt solutions than those studied here also display spectral diffusion times that are faster than the reorientation time.[13] In bulk water, while the orientational relaxation requires jump reorientation, spectral diffusion can occur through the rearrangement of H-bonds of surrounding water molecules bonded to the HOD, which changes the strengths of the H-bonds and therefore the frequency, without the HOD molecule itself undergoing jump reorientation. In a similar vein, recent simulations show that a component of spectral diffusion is associated with breaking and then reforming the same H-bond.[75] The virtually identical slow components of the spectral diffusion and orientational relaxation measured here may be an indication that in these very high concentration salt solutions, the slow spectral diffusion is dominated by reorientation.

The spectral diffusion dynamics of aqueous LiCl solutions over the same range of concentrations were recently measured using the nitrile stretch of MeSCN.[37] This probe was shown to be a good reporter of the water spectral diffusion, reproducing the bulk water spectral diffusion time constants.[38] The spectrum of the CN stretch is very narrow (~ 20 cm^{-1}) and has two peaks, one that arises when water is bound to the N lone pair and the other when Li$^+$ is bound. The CN stretch vibrational lifetime is long, ~ 30 ps, allowing the observation of chemical exchange, that is, water replacing the Li$^+$ bound to N and Li$^+$ replacing water. The time constants for water replacing Li$^+$ range from 92 to 154 ps as the concentration is decreased from 1−4 to 1−6 and those for Li$^+$ replacing water go from 41 to 59 ps.[38]

There are significant differences between the spectral diffusion measured using the CN stretch of MeSCN and the OD stretch of HOD as vibrational probes. The MeSCN probe reported three spectral diffusion decay processes.[37] The first two decay components were thought to be slower versions of the spectral diffusion processes observed in bulk water. While the first time constant (~ 1.2 ps) is very similar for the CN and OD probes, the second time constant is significantly longer for HOD, ~ 13 ps, than it is for MeSCN, 4 ± 1 ps. In addition, MeSCN reported a third, long time component of ~ 40 ps that was not observed with HOD. Within the experimental error, the CN spectral diffusion dynamics was the same regardless of the concentration or which species was bound to the N lone pair. However, the orientational relaxation times of MeSCN with water bound range from ~ 15 to ~ 8 ps as the concentration is reduced from 1−4 to 1−6 and from ~ 54 to ~ 36 ps when Li$^+$ is bound.[38] Therefore, orientational relaxation is not responsible for the spectral diffusion.

A major difference between the interactions of the CN probe and the OD probe with their surroundings is that CN displays a strong, well-documented first-order Stark effect.[39−41] Electric fields produced by the medium have a major effect on the vibrational frequencies of the nitriles. In contrast, the frequencies of the OD stretch mode are dominated by H-bond interactions. For CN, the first spectral diffusion component is likely caused by the H-bond length fluctuations of the species bound to the N lone pair (water or Li$^+$). For the OD of HOD, fluctuations of the H-bond to the chloride cause this component of the spectral diffusion. For the second component, fast fluctuations of the sea of ions and water surrounding MeSCN produce fast electric field fluctuations, which in turn produce frequency fluctuations through first-order Stark coupling. The inhomogeneous distribution of

electric fields will contribute to the portion of the inhomogeneous broadening (Δ_2) associated with the ~ 4 ps time scale. Interactions other than the Stark coupling can also contribute to Δ_2 for MeSCN. For example, simulations of SeCN$^-$ in bulk water showed that interactions with water in different orientations about the CN bond contributed to inhomogeneous broadening and spectral diffusion.[76] The combined fluctuations of the Stark effect and other interactions can result in the ~ 4 ps spectral diffusion time, τ_2. In contrast, the frequency of the OD H-bonded to chloride is mainly sensitive to the H-bonding configuration. The jump reorientation will break and remake new H-bonds producing frequency changes, which occur on a timescale of 13 ± 1 ps.

The third time constant found using the CN probe is ~ 40 ps and is independent of concentration within the relatively large error bars.[37] The CN stretch of MeSCN has a much longer lifetime (~ 30 ps) than the OD stretch of HOD (~ 5 ps). The short lifetime of the HOD probe could prevent the observation of the longest spectral diffusion component. However, we found that the inclusion of a third slow component in the CLS decay of HOD or an offset did not improve the fit to the data. The Akaike statistical test was used to determine if a triexponential function produced a statistically significant improvement in the fit compared to the biexponential decay. The results showed that the biexponential fit is substantially preferred over the triexponential model.

The ~ 40 ps component was ascribed to first-order Stark coupling to the fluctuating electric fields produced by the water−ion network, implying that this is the time constant for the complete randomization of the network. As mentioned above, and shown in several simulation studies,[77−79] other types of intermolecular interactions in addition to Stark coupling can contribute to inhomogeneous broadening and spectral diffusion. Here, we compared spectral diffusion measured by two vibrational probes in identical LiCl solutions, MeSCN, which has strong first-order Stark coupling, and HOD, which does not. The absence of the long time constant from the decays observed with HOD supports the assignment[37] of the long time component of the MeSCN spectral diffusion to the randomization of the water−ion network.

4. CONCLUDING REMARKS

We have investigated the effects of very high LiCl concentrations on the structure and dynamics of water-in-salt solutions through the use of the OD stretch of isotopically dilute HOD as a vibrational probe. At these concentrations, the presence of ion pairing and clustering is significant, resulting in a continuous network of water−ion structures. This structural organization produces substantial changes in the properties of the medium compared to bulk water and low concentration salt solutions.

Vibrational relaxation, which is sensitive to the coupling of the vibrational mode of the probe to its local environment, was used to separate the OD stretch absorption spectrum into contributions from water−water and water−anion interactions. From this, the average H-bond strength of these interactions can be determined from the center frequency of the corresponding spectra. While the chloride-associated population was shifted to higher frequencies (weaker H-bonds than bulk water), in agreement with previous experiments, it was found that the water-associated population was notably shifted to lower frequencies, indicating that the water−water H-bond interaction in concentrated LiCl solutions is on average

stronger than that in bulk water. The enhanced H-bond strength of these interactions, in response to the high salt content in solution, has an impact on water's properties such as viscosity and diffusion. The configuration of the ions near the interacting water molecules affects the partial charges of the H-bond donor and H-acceptor in a manner which strengthens the H-bonds.[62]

Through careful analysis of the anisotropy, reorientation dynamics and angular restriction about the intact water H-bond were observed. At the LiCl concentrations studied, it was found that there is a wide range of dynamics and angular restriction, which vary with the OD stretch frequency. The dynamics and restriction were quantified using the wobbling-in-a-cone model, which gave the restricted diffusion constants and wobbling cone angles. More strongly H-bonded water molecules showed much slower diffusion and more angular restriction. The magnitude and frequency dependence of the restrictions decreased as the molar ratio was reduced from 1−4 to 1−6, becoming almost frequency-independent at the lowest concentration. These observations can be rationalized as increased steric hindrance from the structural ordering induced by the ions. The wobbling cone angles increase at all frequencies studied as the water content increases, as a result of structures less crowded with ions. The rigid structures imparted by the ions have a particularly notable effect on more strongly H-bonded waters, similar to the results obtained from the vibrational relaxation measurements.

The spectral diffusion dynamics (structural fluctuations) observed by the OD stretch of HOD in the LiCl solutions were also measured using 2D IR spectroscopy. In bulk water, spectral diffusion has a fast time scale from the local fluctuations of the H-bond length and a slower time scale from the breaking and making of H-bonds, leading to the complete randomization of the water H-bond network. In the LiCl solutions, these processes are significantly slower than in bulk water and dilute salt solutions. While the time constants for the two processes showed no change with the salt content within the experimental error at these concentrations, the frequency fluctuation amplitudes indicated that the H-bond reorganization plays a more dominant role in the inhomogeneous broadening of the vibrational mode as the salt concentration increases. The slow component of the spectral diffusion, ~13 ps, is essentially identical to the time for complete orientational relaxation measured from the PSPP experiments. The near identity of the slow component of the spectral diffusion and the complete reorientation time suggests that this spectral diffusion component reflects rearrangement of water molecules in the water−ion network.

In summary, we have provided detailed insights into the influence of water−ion networks on the dynamics and structure of water in very concentrated LiCl solutions. These experiments provide a step toward understanding water−ion, ion−ion, and water−water interactions in water-in-salt electrolytes. Previous experiments and simulations on specific cations and anions have reported trends in the angular restriction and the H-bond strength.[12,13,62] However, the frequency dependence of the cone angles and the H-bond strength at high concentrations have not been thoroughly investigated. In future experiments, the more rigorous analyses used in this study will be applied to other highly concentrated salt solutions. The concentration range of LiCl will also be extended and ab initio MD simulations (currently in progress)

will be used to obtain increased molecular level information on structure and dynamics.

■ AUTHOR INFORMATION

Corresponding Author

Michael D. Fayer − *Department of Chemistry, Stanford University, Stanford, California 94305, United States;* ⓘ orcid.org/0000-0002-0021-1815; Phone: (650) 723-4446; Email: fayer@stanford.edu

Authors

Sean A. Roget − *Department of Chemistry, Stanford University, Stanford, California 94305, United States;* ⓘ orcid.org/0000-0003-2470-3571

Kimberly A. Carter-Fenk − *Department of Chemistry, Stanford University, Stanford, California 94305, United States;* ⓘ orcid.org/0000-0003-0071-7127

Complete contact information is available at:
https://pubs.acs.org/10.1021/jacs.2c00616

Notes

The authors declare no competing financial interest.
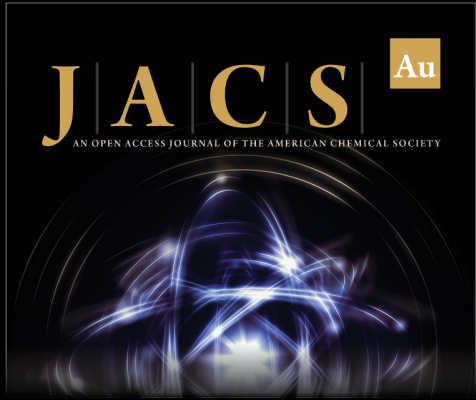
■ REFERENCES

(1) Marcus, Y. Effect of Ions on the Structure of Water: Structure Making and Breaking. *Chem. Rev.* **2009**, *109*, 1346−1370.

(2) Terpstra, P.; Combes, D.; Zwick, A. Effect of salts on dynamics of water: A Raman spectroscopy study. *J. Chem. Phys.* **1990**, *92*, 65−70.

(3) Chizhik, B. V. I. NMR relaxation and microstructure of aqueous electrolyte solutions. *Mol. Phys.* **1997**, *90*, 653−659.

(4) Cota, R.; Ottosson, N.; Bakker, H. J.; Woutersen, S. Evidence for Reduced Hydrogen-Bond Cooperativity in Ionic Solvation Shells from Isotope-Dependent Dielectric Relaxation. *Phys. Rev. Lett.* **2018**, *120*, No. 216001.

(5) Harsányi, I.; Pusztai, L. Hydration structure in concentrated aqueous lithium chloride solutions: A reverse Monte Carlo based combination of molecular dynamics simulations and diffraction data. *J. Chem. Phys.* **2012**, *137*, 204503.

(6) Park, S.; Fayer, M. D. Hydrogen bond dynamics in aqueous NaBr solutions. *Proc. Natl. Acad. Sci. U. S. A.* **2007**, *104*, 16731−16738.

(7) Bakker, H. J. Structural Dynamics of Aqueous Salt Solutions. *Chem. Rev.* **2008**, *108*, 1456−1473.

(8) Moilanen, D. E.; Wong, D.; Rosenfeld, D. E.; Fenn, E. E.; Fayer, M. D. Ion-water hydrogen-bond switching observed with 2D IR vibrational echo chemical exchange spectroscopy. *Proc. Natl. Acad. Sci. U. S. A.* **2009**, *106*, 375−380.

(9) Ji, M. B.; Odelius, M.; Gaffney, K. J. Large Angular Jump Mechanism Observed for Hydrogen Bond Exchange in Aqueous Perchlorate Solution. *Science* **2010**, *328*, 1003−1005.

(10) Tielrooij, K. J.; van der Post, S. T.; Hunger, J.; Bonn, M.; Bakker, H. J. Anisotropic Water Reorientation around Ions. *J. Phys. Chem. B* **2011**, *115*, 12638.

(11) Tielrooij, K. J.; van der Post, S. T.; Hunger, J.; Bonn, M.; Bakker, H. J. Cooperativity in Ion Hydration. *J. Phys. Chem. B* **2011**, *115*, 12638−12647.

(12) van der Post, S. T.; Bakker, H. J. The combined effect of cations and anions on the dynamics of water. *Phys. Chem. Chem. Phys.* **2012**, *14*, 6280−6288.

(13) Giammanco, C. H.; Wong, D. B.; Fayer, M. D. Water Dynamics in Divalent and Monovalent Concentrated Salt Solutions. *J. Phys. Chem. B* **2012**, *116*, 13781−13792.

(14) Wei, Q.; Zhou, D.; Bian, H. Negligible cation effect on the vibrational relaxation dynamics of water molecules in NaClO4 and LiClO4 aqueous electrolyte solutions. *RSC Adv.* **2017**, *7*, 52111−52117.

(15) Bian, H.; Wen, X.; Li, J.; Chen, H.; Han, S.; Sun, X.; Song, J.; Zhuang, W.; Zheng, J. Ion clustering in aqueous solutions probed with vibrational energy transfer. *Proc. Natl. Acad. Sci. U. S. A.* **2011**, *108*, 4737−4742.

(16) Sun, Z.; Zhang, W.; Ji, M.; Hartsock, R.; Gaffney, K. J. Contact Ion Pair Formation between Hard Acids and Soft Bases in Aqueous Solutions Observed with 2DIR Spectroscopy. *J. Phys. Chem. B* **2013**, *117*, 15306−15312.

(17) van der Vegt, N. F. A.; Haldrup, K.; Roke, S.; Zheng, J.; Lund, M.; Bakker, H. J. Water-Mediated Ion Pairing: Occurrence and Relevance. *Chem. Rev.* **2016**, *116*, 7626−7641.

(18) Fournier, J. A.; Carpenter, W.; De Marco, L.; Tokmakoff, A. Interplay of Ion−Water and Water−Water Interactions within the Hydration Shells of Nitrate and Carbonate Directly Probed with 2D IR Spectroscopy. *J. Am. Chem. Soc.* **2016**, *138*, 9634−9645.

(19) Lim, J.; Park, K.; Lee, H.; Kim, J.; Kwak, K.; Cho, M. Nanometric Water Channels in Water-in-Salt Lithium Ion Battery Electrolyte. *J. Am. Chem. Soc.* **2018**, *140*, 15661−15667.

(20) Lewis, N. H. C.; Zhang, Y.; Dereka, B.; Carino, E. V.; Maginn, E. J.; Tokmakoff, A. Signatures of Ion Pairing and Aggregation in the Vibrational Spectroscopy of Super-Concentrated Aqueous Lithium Bistriflimide Solutions. *J. Phys. Chem. C* **2020**, *124*, 3470−3481.

(21) Zhang, M.; Hao, H.; Zhou, D.; Duan, Y.; Wang, Y.; Bian, H. Understanding the Microscopic Structure of a "Water-in-Salt" Lithium Ion Battery Electrolyte Probed with Ultrafast IR Spectroscopy. *J. Phys. Chem. C* **2020**, *124*, 8594−8604.

(22) Suo, L.; Borodin, O.; Gao, T.; Olguin, M.; Ho, J.; Fan, X.; Luo, C.; Wang, C.; Xu, K. "Water-in-salt" electrolyte enables high-voltage aqueous lithium-ion chemistries. *Science* **2015**, *350*, 938−943.

(23) Yamada, Y.; Usui, K.; Sodeyama, K.; Ko, S.; Tateyama, Y.; Yamada, A. Hydrate-melt electrolytes for high-energy-density aqueous batteries. *Nat. Energy* **2016**, *1*, 16129.

(24) Li, M.; Wang, C.; Chen, Z.; Xu, K.; Lu, J. New Concepts in Electrolytes. *Chem. Rev.* **2020**, *120*, 6783−6819.

(25) Suo, L.; Borodin, O.; Wang, Y.; Rong, X.; Sun, W.; Fan, X.; Xu, S.; Schroeder, M. A.; Cresce, A. V.; Wang, F.; Yang, C.; Hu, Y.-S.; Xu, K.; Wang, C. "Water-in-Salt" Electrolyte Makes Aqueous Sodium-Ion Battery Safe, Green, and Long-Lasting. *Adv. Energy Mater.* **2017**, *7*, No. 1701189.

(26) Wang, F.; Borodin, O.; Gao, T.; Fan, X.; Sun, W.; Han, F.; Faraone, A.; Dura, J. A.; Xu, K.; Wang, C. Highly reversible zinc metal anode for aqueous batteries. *Nat. Mat.* **2018**, *17*, 543−549.

(27) Zhao, J.; Li, Y.; Peng, X.; Dong, S.; Ma, J.; Cui, G.; Chen, L. High-voltage Zn/LiMn$_{0.8}$Fe$_{0.2}$PO$_4$ aqueous rechargeable battery by virtue of "water-in-salt" electrolyte. *Electrochem. Commun.* **2016**, *69*, 6−10.

(28) Johnston, C. T.; Agnew, S. F.; Schoonover, J. R.; Kenney, J. W.; Page, B.; Osborn, J.; Corbin, R. Raman Study of Aluminum Speciation in Simulated Alkaline Nuclear Waste. *Environ. Sci. Technol.* **2002**, *36*, 2451−2458.

(29) Sipos, P. The structure of Al(III) in strongly alkaline aluminate solutions — A review. *J. Mol. Liq.* **2009**, *146*, 1−14.

(30) Reynolds, J. G.; Cooke, G. A.; Herting, D. L.; Warrant, R. W. Salt Mineralogy of Hanford High-Level Nuclear Waste Staged for Treatment. *Ind. Eng. Chem. Res.* **2013**, *52*, 9741−9751.

(31) Soper, A. K. The radial distribution functions of water and ice from 220 to 673 K and at pressures up to 400 MPa. *Chem. Phys.* **2000**, *258*, 121−137.

(32) Prendergast, D.; Galli, G. X-Ray Absorption Spectra of Water from First Principles Calculations. *Phys. Rev. Lett.* **2006**, *96*, No. 215502.

(33) Marcus, Y.; Hefter, G. Ion Pairing. *Chem. Rev.* **2006**, *106*, 4585−4621, DOI: 10.1021/cr040087x.

(34) Singh, M. B.; Dalvi, V. H.; Gaikar, V. G. Investigations of clustering of ions and diffusivity in concentrated aqueous solutions of lithium chloride by molecular dynamic simulations. *RSC Adv.* **2015**, *5*, 15328−15337.

(35) Pethes, I. The structure of aqueous lithium chloride solutions at high concentrations as revealed by a comparison of classical interatomic potential models. *J. Mol. Liq.* **2018**, *264*, 179−197.

(36) Ibuki, K.; Bopp, P. A. Molecular dynamics simulations of aqueous LiCl solutions at room temperature through the entire concentration range. *J. Mol. Liq.* **2009**, *147*, 56−63.

(37) Yuan, R.; Fayer, M. D. Dynamics of Water Molecules and Ions in Concentrated Lithium Chloride Solutions Probed with Ultrafast 2D IR Spectroscopy. *J. Phys. Chem. B* **2019**, *123*, 7628−7639.

(38) Yuan, R.; Yan, C.; Fayer, M. Ion−Molecule Complex Dissociation and Formation Dynamics in LiCl Aqueous Solutions from 2D IR Spectroscopy. *J. Phys. Chem. B* **2018**, *122*, 10582−10592.

(39) Andrews, S. S.; Boxer, S. G. Vibrational stark effects of nitriles I. Methods and experimental results. *J. Phys. Chem. A* **2000**, *104*, 11853−11863.

(40) Williams, R. B.; Loring, R. F.; Fayer, M. D. Vibrational Dephasing of Carbonmonoxy Myoglobin. *J. Phys. Chem. B* **2001**, *105*, 4068−4071.

(41) Bagchi, S.; Boxer, S. G.; Fayer, M. D. Ribonuclease S dynamics measured using a nitrile label with 2D IR vibrational echo spectroscopy. *J. Phys. Chem. B* **2012**, *116*, 4034−4042.

(42) Fenn, E. E.; Wong, D. B.; Fayer, M. D. Water Dynamics in Small Reverse Micelles in Two Solvents: Two-Dimensional Infrared Vibrational Echoes with Two-Dimensional Background Subtraction. *J. Chem. Phys.* **2011**, *134*, No. 054512.

(43) Steinel, T.; Asbury, J. B.; Zheng, J. R.; Fayer, M. D. Watching hydrogen bonds break: A transient absorption study of water. *J. Phys. Chem. A* **2004**, *108*, 10957−10964.

(44) Rezus, Y. L. A.; Bakker, H. J. On the orientational relaxation of HDO in liquid water. *J. Chem. Phys.* **2005**, *123*, 114502.

(45) Kwak, K.; Park, S.; Finkelstein, I. J.; Fayer, M. D. Frequency-frequency correlation functions and apodization in two-dimensional infrared vibrational echo spectroscopy: A new approach. *J. Chem. Phys.* **2007**, *127*, 124503.

(46) Kwak, K.; Rosenfeld, D. E.; Fayer, M. D. Taking apart the two-dimensional infrared vibrational echo spectra: More information and elimination of distortions. *J. Chem. Phys.* **2008**, *128*, 204505.

(47) Guo, Q.; Pagano, P.; Li, Y.-L.; Kohen, A.; Cheatum, C. M. Line shape analysis of two-dimensional infrared spectra. *J. Chem. Phys.* **2015**, *142*, 212427.

(48) Bergström, P.-A.; Lindgren, J.; Kristiansson, O. An IR Study of the Hydration of ClO$_4^−$, NO$_3^−$, I$^−$, Br$^−$, Cl$^−$, and SO$_4^{2−}$ Anions in Aqueous Solution. *J. Phys. Chem.* **1991**, *95*, 8575−8580.

(49) Kropman, M. F.; Bakker, H. J. Vibrational relaxation of liquid water in ionic solvation shells. *Chem. Phys. Lett.* **2003**, *370*, 741−746.

(50) Smith, J. D.; Saykally, R. J.; Geissler, P. L. The Effect of Dissolved Halide Anions on Hydrogen Bonding in Liquid Water. *J. Am. Chem. Soc.* **2007**, *129*, 13847−13856.

(51) Kristiansson, O.; Lindgren, J. On the hydration of the F− anion in aqueous solution. *J. Mol. Struct.* **1988**, *177*, 537−541.

(52) Stangret, J.; Gampe, T. Hydration Sphere of Tetrabutylammonium Cation. FTIR Studies of HDO Spectra. *J. Phys. Chem. B* **1999**, *103*, 3778−3783.

(53) Nickolov, Z. S.; Miller, J. D. Water structure in aqueous solutions of alkali halide salts: FTIR spectroscopy of the OD stretching band. *J. Colloid Interface Sci.* **2005**, *287*, 572−580.

(54) Kramer, P. L.; Giammanco, C. H.; Fayer, M. D. Dynamics of water, methanol, and ethanol in a room temperature ionic liquid. *J. Chem. Phys.* **2015**, *142*, 212408.

(55) Giammanco, C. H.; Kramer, P. L.; Fayer, M. D. Ionic Liquid versus Li+ Aqueous Solutions: Water Dynamics near Bistriflimide Anions. *J. Phys. Chem. B* **2016**, *120*, 9997−10009.

(56) Śmiechowski, M.; Gojło, E.; Stangret, J. Ionic Hydration in LiPF6, NaPF6, and KPF6 Aqueous Solutions Derived from Infrared HDO Spectra. *J. Phys. Chem. B* **2004**, *108*, 15938−15943.

(57) Nam, D.; Lee, C.; Park, S. Temperature-dependent dynamics of water in aqueous NaPF6 solution. *Phys. Chem. Chem. Phys.* **2014**, *16*, 21747−21754.

(58) Giammanco, C. H.; Kramer, P. L.; Wong, D. B.; Fayer, M. D. Water Dynamics in 1-Alkyl-3-methylimidazolium Tetrafluoroborate Ionic Liquids. *J. Phys. Chem. B* **2016**, *120*, 11523−11538.

(59) Kenkre, V. M.; Tokmakoff, A.; Fayer, M. D. Theory of Vibrational Relaxation of Polyatomic Molecules in Liquids. *J. Chem. Phys.* **1994**, *101*, 10618−10629.

(60) Timmer, R. L. A.; Bakker, H. J. Vibrational Förster Transfer in Ice Ih. *J. Phys. Chem. A* **2010**, *114*, 4148−4155.

(61) Perakis, F.; Hamm, P. Two-dimensional infrared spectroscopy of neat ice Ih. *Phys. Chem. Chem. Phys.* **2012**, *14*, 6250−6256.

(62) Zeng, Y.; Jia, Y.; Yan, T.; Zhuang, W. Binary structure and dynamics of the hydrogen bonds in the hydration shells of ions. *Phys. Chem. Chem. Phys.* **2021**, *23*, 11400−11410.

(63) Laage, D.; Hynes, J. T. A Molecular Jump Mechanism of Water Reorientation. *Science* **2006**, *311*, 832−835.

(64) Moilanen, D. E.; Fenn, E. E.; Lin, Y. S.; Skinner, J. L.; Bagchi, B.; Fayer, M. D. Water inertial reorientation: Hydrogen bond strength and the angular potential. *Proc. Natl. Acad. Sci. U. S. A.* **2008**, *105*, 5295−5300.

(65) Kinosita, K.; Kawato, S.; Ikegami, A. Theory of Fluorescence Polarization Decay in Membranes. *Biophys. J.* **1977**, *20*, 289−305.

(66) Kinosita, K.; Ikegami, A.; Kawato, S. On the wobbling-in-cone analysis of fluorescence anisotropy decay. *Biophys. J.* **1982**, *37*, 461−464.

(67) Lipari, G.; Szabo, A. Effect of Librational Motion on Fluorescence Depolarization and Nuclear Magnetic-Resonance Relaxation in Macromolecules and Membranes. *Biophys. J.* **1980**, *30*, 489−506.

(68) Hoffman, D. J.; Fica-Contreras, S. M.; Fayer, M. D. Amorphous polymer dynamics and free volume element size distributions from ultrafast IR spectroscopy. *Proc. Natl. Acad. Sci. U. S. A.* **2020**, *117*, 13949−13958.

(69) Fica-Contreras, S. M.; Hoffman, D. J.; Pan, J.; Liang, C.; Fayer, M. D. Free Volume Element Sizes and Dynamics in Polystyrene and Poly(methyl methacrylate) Measured with Ultrafast Infrared Spectroscopy. *J. Am. Chem. Soc.* **2021**, *143*, 3583−3594.

(70) Kubo, R. A Stochastic Theory of Line-Shape and Relaxation. In *Fluctuation, Relaxation and Resonance in Magnetic Systems*; Ter Haar, D., Ed.; Oliver and Boyd: London, 1961.

(71) Hamm, P.; Zanni, M. T. *Concepts and Methods of 2D Infrared Spectroscopy*; Cambridge University Press: Cambridge; New York, 2011.

(72) Hoffman, D. J.; Fayer, M. D. CLS Next Gen: Accurate Frequency−Frequency Correlation Functions from Center Line Slope Analysis of 2D Correlation Spectra Using Artificial Neural Networks. *J. Phys. Chem. A* **2020**, *124*, 5979−5992.

(73) Asbury, J. B.; Steinel, T.; Kwak, K.; Corcelli, S. A.; Lawrence, C. P.; Skinner, J. L.; Fayer, M. D. Dynamics of Water Probed with Vibrational Echo Correlation Spectroscopy. *J. Chem. Phys.* **2004**, *121*, 12431.

(74) Asbury, J. B.; Steinel, T.; Stromberg, C.; Corcelli, S. A.; Lawrence, C. P.; Skinner, J. L.; Fayer, M. D. Water Dynamics: Vibrational Echo Correlation Spectroscopy and Comparison to Molecular Dynamics Simulations. *J. Phys. Chem. A* **2004**, *108*, 1107−1119.

(75) Piskulich, Z. A.; Laage, D.; Thompson, W. H. On the role of hydrogen-bond exchanges in the spectral diffusion of water. *J. Chem. Phys.* **2021**, *154*, No. 064501.

(76) Yamada, S. A.; Thompson, W. H.; Fayer, M. D. Water-anion hydrogen bonding dynamics: Ultrafast IR experiments and simulations. *J. Chem. Phys.* **2017**, *146*, 234501.

(77) Błasiak, B.; Ritchie, A. W.; Webb, L. J.; Cho, M. Vibrational solvatochromism of nitrile infrared probes: beyond the vibrational Stark dipole approach. *Phys. Chem. Chem. Phys.* **2016**, *18*, 18094−18111.

(78) Daly, C. A.; Berquist, E. J.; Brinzer, T.; Garrett-Roe, S.; Lambrecht, D. S.; Corcelli, S. A. Modeling Carbon Dioxide Vibrational Frequencies in Ionic Liquids: II. Spectroscopic Map. *J. Phys. Chem. B* **2016**, *120*, 12633−12642.

(79) Lewis, N. H. C.; Iscen, A.; Felts, A.; Dereka, B.; Schatz, G. C.; Tokmakoff, A. Vibrational Probe of Aqueous Electrolytes: The Field Is Not Enough. *J. Phys. Chem. B* **2020**, *124*, 7013−7026.